Comput. & Graphics Vol. 17, No. 6, pp. 643–653, 1993
Printed in Great Britain.

0097-8493/93 $6.00 + .00

SIMULATING PERIPHERAL VISION IN IMMERSIVE VIRTUAL ENVIRONMENTS

MEL SLATER and MARTIN USOH
Department of Computer Science and London Parallel Applications Centre (LPAC), QMW University of London, Mile End Road, London E1 4NS UK

Abstract—The standard graphics viewing pipeline is designed for images that are to be viewed externally, as on a screen or photograph. It may not be suitable for Immersive Virtual Environments (Virtual Reality) for many different reasons, one being the lack of peripheral vision. Peripheral vision offers important cues for direction of gaze and movement in the environment. This paper presents an alternative (but simple) viewing pipeline, that includes visual cues that could stimulate peripheral vision. After a brief discussion of Immersive Virtual Environments, there is a description of the functioning of peripheral vision. This is followed by an analysis of the standard viewing model of computer graphics and the presentation of an alternative. Implementation details and a simple experiment on peripheral vision are described.

1. INTRODUCTION

A virtual environment (VE) is a dynamic environment that is created by presenting a human observer with a world displayed by computer. The displays provide signals in the visual, auditory, and tactual (tactile, kinesthetic, force-feedback) modalities. In *immersive* VEs (IVEs) sensory input to the human from the external world is supplemented, or wholly taken over, by at least one computer generated display. We include the term "supplemented," since we would also include as IVEs the "see through" type, which merge inputs to the senses from the real world with those that are computer generated[1]. To properly qualify, the merging should be seamless. Thus provision of a stereo display on a 2D screen is not an immersive virtual environment, since the screen itself can be seen.

Following Ellis[2] an environment consists of content, geometry, and dynamics. The content consists of *objects*, a subset of which are *actors*. Objects have specific properties such as position, orientation, velocity and acceleration in space, as well as physical properties such as shape, colour, mass, and so on. Actors are distinguished from objects in that they are capable of initiating an interaction with other actors or objects. The geometry of an environment defines the space in which the objects exist. It consists of a metric, a dimensionality, and an extent. Finally, the dynamic specifies rules of interaction between objects.

In an IVE there is at least one actor that provides the egocentric point from which the environment can be described. This point determines a visual point of view, an auditory location, and a tactual frame of reference, from which the environment can be displayed by the computer. We use the term *display* here to incorporate outputs that provide consistent inputs (ideally) to all of the human senses. This actor *embodies* the human participant, who constructs the world through perception of this display.

Such IVEs, popularly called Virtual Reality (VR), therefore provide a tightly coupled human-computer interface: input to the sensory organs of the human participant are directly generated through computer displays, in the visual, auditory, and tactual modalities. The participant operates in an extended virtual space created by the interaction between the human perceptual system and the computer generated displays. This affords the possibility of participants maintaining a sense of presence in the VE, that is the (suspension of dis-) belief that they are in a world other than where their real bodies are located. This is the unique possibility that IVEs offer: Just as computers are general purpose machines, IVEs may be considered general purpose presence-transforming machines.

In this paper we examine peripheral vision—a particular aspect of the interaction between the human perceptual system and the visual display. In Section 2 we outline the importance of peripheral vision in human visual processing. In Section 3 we describe a simple experiment with users in order to assess whether it is possible to stimulate the effects of peripheral vision at all in IVEs. In Section 4 we show how the standard computer graphics viewing pipeline does not support peripheral vision, and we present a modified viewing pipeline that does incorporate this. In Section 5 we discuss the implementation of the modified pipeline, with results in Section 6. The conclusions are presented in Section 7.

2. PERIPHERAL VISION

Current theories of vision postulate a two phase process—the primary visual system, based on operations mainly in the eye and midbrain regions, and major processing in the visual cortex. Images are focussed onto the retina, which is a very thin tissue (150–300 μm) that lies at the back of the eye. The focussing is achieved through the refractive power of the cornea and lens and the fluids that fill the eye (acqueous and vitreous humor). The retina is transparent, so light passes completely through it before stimulating the photo-receptors at the back of the retina. These photo-receptors are of two types, called rods and cones, there being 120×10^6 rods and 5×10^6 cones. The rods are responsible for vision in poorly illuminated environments, whereas the cones operate in bright light and provide visual acuity and colour.

The distribution of rods and cones is not uniform over the retina. The fovea at the centre of the retina contains the vast majority of cones, and a smaller central area within this contains only cones. It is in this region that visual acuity is maximum, and images formed outside of this region decrease in acuity the further away they are from the centre. From the fovea outwards, the rod density at first increases from zero to 150,000 per mm^2 at 18° from the fovea, and then decreases to less than 40,000 per per mm^2 at the edge. Images that focus on the periphery of the retina are received by the rods alone, which are therefore responsible also for peripheral vision. It should be noted that images in the periphery are not clear[3]. If acuity in the fovea centralis is 20–20, then in the peripheral regions it is of the order 20–400.

Movement detection rather than clarity is an important function of the peripheral regions; events detected in the periphery trigger a change in direction of gaze, causing the eye and/or head to turn towards the direction of the event. A standard textbook on physiology states, "Even after the visual cortex has been destroyed, a sudden visual disturbance in a lateral area of the visual field will cause immediate turning of the eyes in that direction. . . . In addition to causing the eyes to turn towards the visual disturbance, signals are also relayed from the superior colliculi through the *medial longitudinal fasciculus* to other levels of the brain stem to cause turning of the whole head and even of the whole body toward the direction of the disturbance"[4, p. 567]. Cotter writes: "The superior colliculus is involved in integration of a variety of sensory stimuli and mechanisms of attention that are important in eye movements . . . it has been hypothesized that the accessory optic system coordinates head and eye movements so that visual images do not blur as a result of head movement"[3, p. 14]. Bruce and Green write: "In the periphery of the visual field motion serves an orienting function. A flashing or moving light will cause human observers to turn their eyes and/or heads automatically to fixate the object. Such orienting functions may be mediated in part by the superior colliculus"[5, p. 165]. Bruce and Green further point out (p. 51) that such automatic turning to fixate a moving object in peripheral vision is often an unconscious behaviour.

The human visual system has field of view (FOV) approximately 180° (binocular) horizontally and 120° vertically. Figure 1 shows typical visual fields of each eye, mapped out on a perimeter[6, p. 451]. Commercially available head-mounted displays (HMDs) do not achieve anything like this. For example, the authors measured the Virtual Research Flight Helmet™ to have a FOV of approximately 75° in the horizontal and 50° in the vertical, which is superior to many other HMDs. A wider FOV can be achieved by reducing the extent of binocular overlap of the images presented to each eye. However, experimental evidence suggests[7] that making the extent of overlap less than 100% decreases the level of performance, for example, in visual search tasks. Therefore, for the foreseeable future HMDs are likely to impose a great loss in peripheral vision for participants in IVEs. The effects of this on performance, and sense of presence are unknown, although [8] reports that immersion requires at least a 60° FOV.

The work of the present authors to date has concentrated on factors influencing the sense of presence in architectural walkthrough applications[9–11]. In particular, we have concentrated on the influence of bestowing a virtual body (VB) on participants, which is of particular importance in the architectural walkthrough context. Our pilot experiments have suggested strongly that the VB does play a significant role in enhancing participants' sense of presence. This is slightly surprising since the relatively small FOV implies that most of the time subjects in the experiments were not visually aware of their VB, although the VB would come into view at crucial moments—for example, while they were reaching or bending to select an object (Figs. 2 and 3). In order to overcome this problem, the experimenters had to supply verbal instructions to subjects to look all around and up and down, at the start of each experimental scenario so that those in the experimental group would become aware that they had a VB. Our verbal instructions were in place of the visual

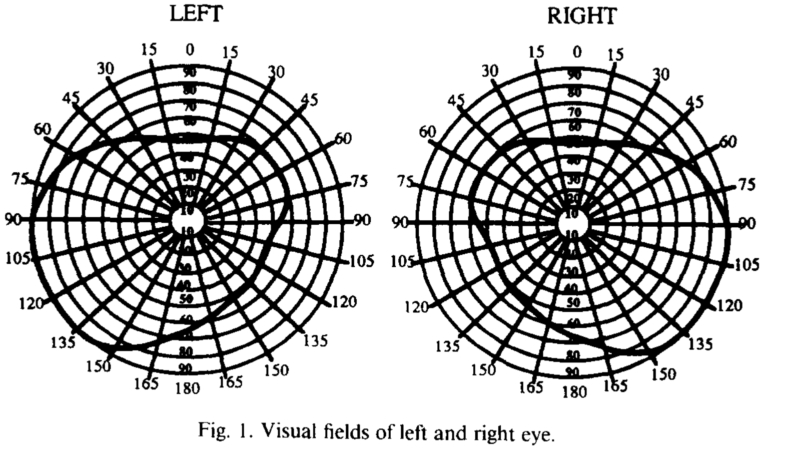

Fig. 1. Visual fields of left and right eye.

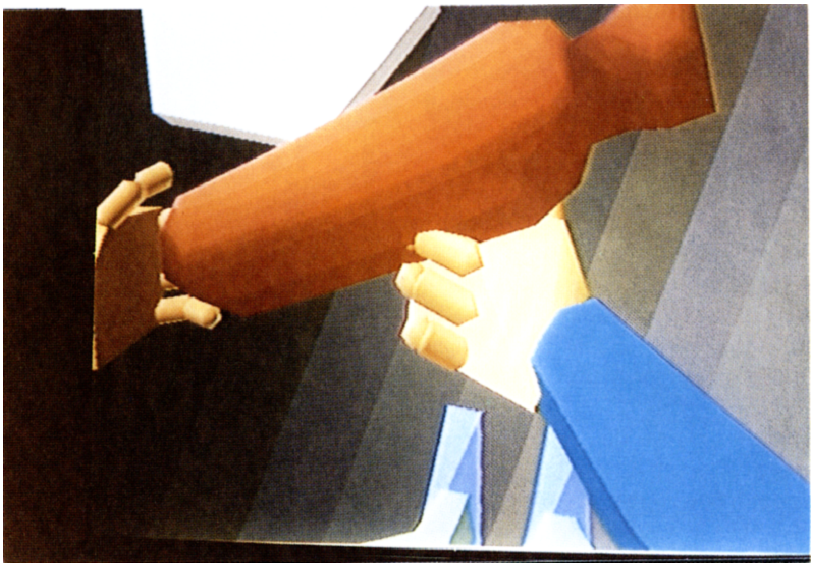

Fig. 2. The hands and feet become visible while the participant lifts an object.

cues that would normally be available in everyday reality—since we are peripherally, if unconsciously, visually aware of our bodies at most times.

3. A SIMPLE EXPERIMENT

In order to assess whether it is possible to stimulate peripheral vision at all in IVEs we carried out a very simple experiment. For this we used the ProVision200 system, a DIVISION 3D mouse (the input device), and a Virtual Research Flight Helmet™ as the head mounted display (HMD). Five subjects were each in turn entered into an identical scenario that showed a house in the distance. They were not allowed to move around, but were able to look in any direction.

Their period in the VE (approximately 3 minutes per subject) was divided into two phases. In the first phase, from the point of view of the subject, nothing happened, they were free to look around the environment. However, at five pre-assigned intervals, data were recorded on the direction of their gaze, each time over a 5-second period. In the second phase, again at pre-assigned intervals, a small cube was displayed at the extreme right-hand edge of their view, approximately at eye level. Each cube was displayed for 5 seconds and then disappeared. The successive cubes were different colours. During the 5 second intervals, data were recorded on the direction of gaze.

A transformation was established, so that the cubes were always shown with direction vector (1, 0, 0). If the subjects were stimulated to look in the direction of the cubes, then we would expect the (X, Y, Z) vec-

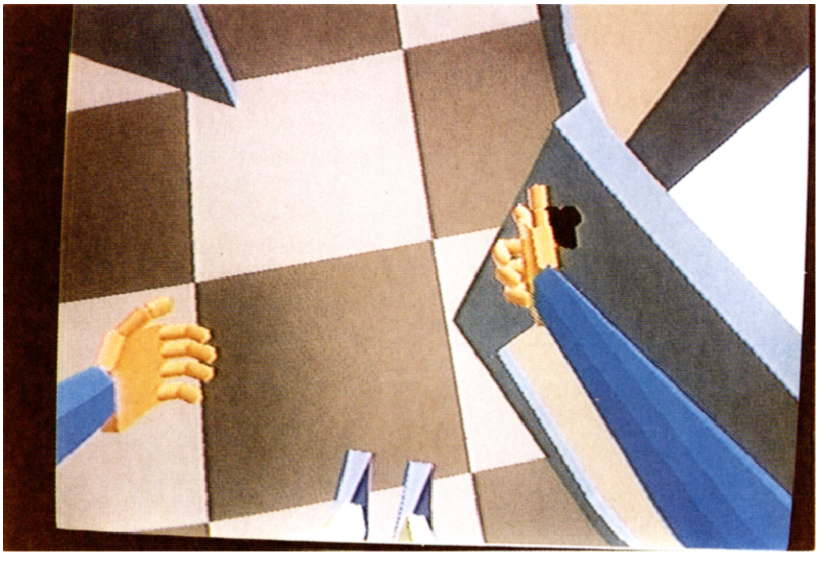

Fig. 3. The body becomes visible while the participant bends to open a cupboard.

tors to be different over the control and experimental periods.

As a matter of direct observation of the subjects, four out of five of them always turned in the direction of the cube when it appeared. The remaining subject turned in the direction of the cube two times out of the five. Figure 4a,b shows the (X, Y, Z) plots for a subject, in a control and experimental period. It shows that during the experimental period there is a clear peak in the X direction coordinate, as the subject turned her head towards the box and then away again. There is no similar peak in the control graph. These graphs illustrate the typical response for four of the five subjects.

The implementation used for this experiment was *ad hoc;* it did not provide a full view of the periphery, nor did it include optic flow in the periphery. Its purpose was to see whether it was possible to stimulate peripheral vision at all given the limitations of today's IVE display technology. The results suggested that for the equipment and scenario we were using, that the effect can be achieved in an IVE. In the following sections a viewing model is proposed that may offer a general purpose solution.

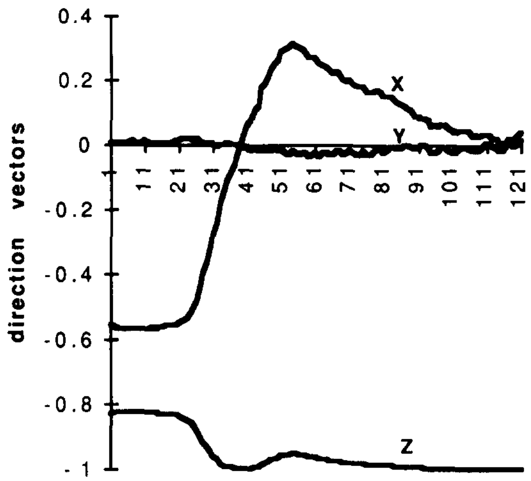

Fig. 4b. Graph of (x, y, z) coordinates for an experimental period.

making the box narrower, that is, moving the view plane nearer to the aperture. However, the effect of this would also be to uniformly scale the image to a smaller size.

4. VIEWING MODEL

4.1. *Pin-hole camera*

Virtual reality systems employ the standard computer graphics viewing pipeline, though with adjustments that take account of the HMD optics (see for example, [12, 13]). The standard computer graphics pipeline is a simulation of the "pin-hole camera," shown in Fig. 5. A light protected box has photographic film on one of the inside faces (call this face the view plane). The opposite face has a tiny aperture that admits light. After a long exposure time an inverted image of the scene will form on the photographic film. The image will have uniform clarity. The FOV is demarcated as the infinite pyramid in object space, with apex at the aperture. It has four bounding planes formed from rays from the corners of the view plane through the aperture. Obviously, the FOV can be increased by

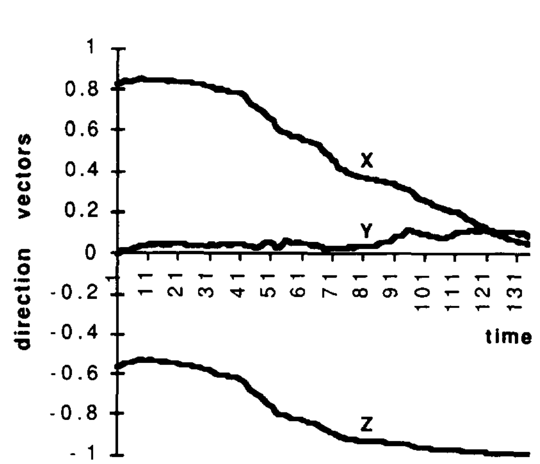

Fig. 4a. Graph of (x, y, z) coordinates for a control period.

4.2. *Standard viewing model*

The standard viewing model was first given full expression in the CORE standard[14] and modified versions adopted for the GKS-3D and PHIGS standards[15], see also [16]. This is illustrated in Fig. 6. In World Coordinates a View Reference Point (VRP) is specified, which is to become the origin of a view-centred coordinate system. The Z (or N) axis of this Viewing Coordinate system is specified by the View Plane Normal (VPN), and the Y (or V) axis may be derived from a View Up Vector (VUV). The X (or U) axis is chosen so as to form a right- or left-handed system as desired[†]. The Centre of Projection (COP) is chosen in Viewing Coordinates (and hence as an offset from the VRP). A view plane (VP) is determined by the View Plane Distance (VPD) along the VPN, measured from the VRP. It is, of course, perpendicular to the VPN.

Rays from an object converge at the COP. The image is formed by their intersection with the VP. A View Plane Window is chosen as an axis-aligned rectangle on the VP. Rays from the corners of the window through the COP specify the view volume. This may be further truncated by near and far clipping planes. The near clipping plane is really a necessity, in order to avoid the anomalies that occur when objects are behind the COP. This set-up is clearly a simulation (and generalisation) of the pin-hole camera, where the COP plays the role of the aperture and the view plane is the photographic film. In this model, however, the image is not inverted.

[†] In this paper the convention is adopted of right-handed World Coordinate system and left-handed coordinate systems for all other frames.

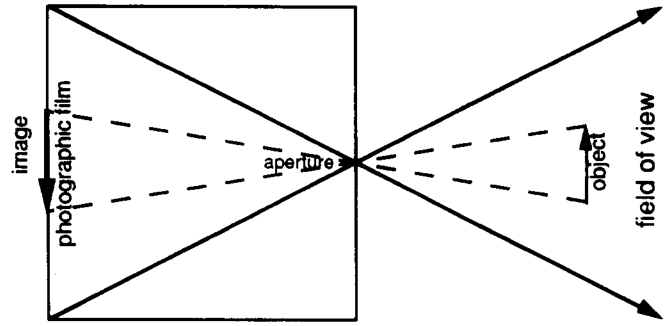

Fig. 5. Pin-hole camera model.

The view volume provides a restricted FOV. This may be increased by increasing the size of the VP window, or by moving the COP closer to the VP. However, in each case the image is reduced in size. Note that the VP window is essentially a floating point and scaled version of the 2D display onto which the image is finally rendered.

4.3. *An alternative model*

The standard viewing model is suitable for applications where the user is concerned with looking *at* a screen, or resulting photograph. For IVEs, however, it is inappropriate in two respects: first, and maybe of less importance is that an image of uniform clarity is rendered onto the display, unless some special effort is made to overcome this. Second, peripheral vision is only possible through reducing the overall size of the image, or by using a fish-eye view. In Section 2, arguments were given as to the importance of peripheral vision in human visual processing, being responsible for triggering changes in direction of gaze. In IVEs visual input to the human is entirely a function of the computer generated displays (except in the case of see-through systems, which have a different set of problems). The deletion of peripheral vision may have important consequences for human functioning in IVEs, and this section offers a modification of the standard view that does attempt to simulate peripheral vision, and identifies portions of the image that may be rendered with differing attention to detail.

A possible solution to the problem could be to project the image on to a hemisphere, followed by a mapping onto a plane. This shown in Fig. 7. Clearly a wide FOV can be maintained. The difficulty here is that the fundamental property of planar perspective projections is lost, the image of a straight line is no longer straight and therefore a large number of points on each line would need to be projected, which is too costly for today's systems.

The criteria we adopt for an alternative model are that:

- it affords peripheral vision;
- it determines areas of the display in the periphery that do not need to be rendered at the highest quality;
- it is computationally no more expensive than the current viewing model;
- it is a modification of current practice rather than a complete overhaul, and therefore compatible with today's hardware and software.

The equivalent to the pin-hole arrangement for such a new model is shown in Fig. 8. Imagine that the camera were not a box, but itself a pyramid truncated in two places. The front view is shown in Figure 8a. A small aperture is placed on the front (larger) face of the "camera," and each of the five other inside faces

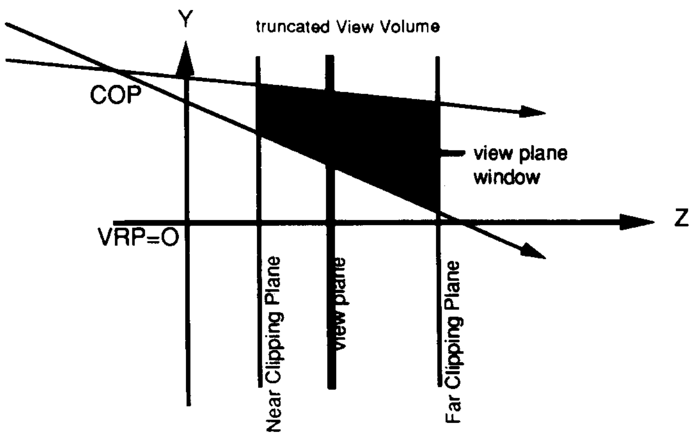

Fig. 6. The standard viewing model.

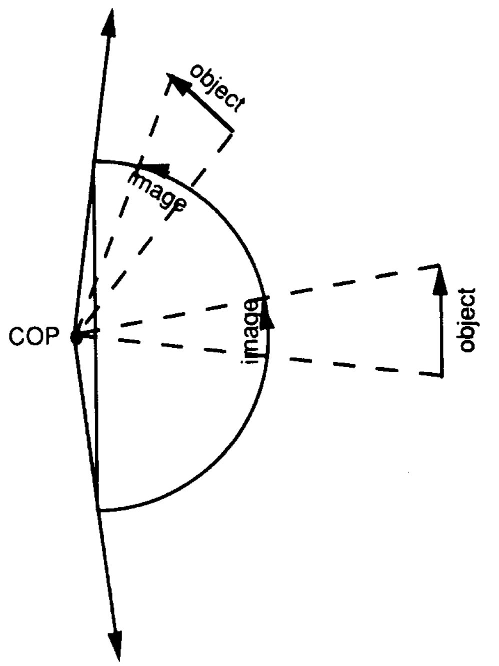

Fig. 7. Projecting onto a sphere: Preserves periphery.

are coated with photographic film. The face directly opposite the aperture will develop a view exactly the same as the standard pin-hole, with its FOV as shown in Fig. 8b. However, the remaining four faces will contain exposures of the periphery. An observer looking at the developed film, constructed in the same physical arrangement, with a viewing direction perpendicular to the front face, will see the undistorted central area in normal perspective, and the periphery subject to a distortion (since it would be observed at acute angles). The combined view will contain an image of the entire scene that is in front of the camera.

This arrangement can be turned into a model analogous to the standard computer graphics model, as shown in Fig. 9. This shows a side view of the doubly truncated pyramid. The COP is located in the centre of the back plane window, denoted by DA in the diagram. The remaining five faces are view planes, with a side view of three of these shown in the 2D plan view as AB, BC, and CD. BC is the usual view plane of computer graphics. A point such as P is projected to the view plane at P′, by a ray through the COP. The difference here is that we now consider the back plane window (AD) as a scaled version of the display, rather than the view plane window (BC). Hence there is a further parallel projection from P' to P'', and P'' is essentially a point on the display. Similarly the point Q is projected to Q', and then again projected onto the back plane at the point Q''. The planes defined by the COP and the corners of the front viewing plane (BC) define the usual FOV (view volume). However, here the peripheral information is also captured, and projected to the view planes that are above, to the right, below, and to the left of this central window. The effect will be that the central region of the final image (shown as EF) will form the usual perspective projection. However, there will be an outer band around this (AF and ED) with distorted images of the periphery.

A near clipping plane can be located anywhere in front of the back plane (indeed it could be the back plane itself, with some care in the projection computations). A far clipping plane can be used if required. There is no need for the four remaining clipping planes defined by the rays from the COP through the (front) view plane window since this clipping is no longer performed. Hence the entire 180° FOV can be rendered.

Figure 10 shows a more general example of such a viewing model, illustrating that the shape is not restricted to a truncation of a regular pyramid. In addition to the usual model we need to specify the back plane window ($x_1 < x_2$, $y_1 < y_2$). However, for simplicity here, we do assume that $x_1 + x_2 = y_1 + y_2 = 0$, in other words, the back plane window must be symmetrical about the COP at the origin. For the new model, the VRP, VUV, VPN, COP, VP distance, and VP window, all have the same meaning as before. The

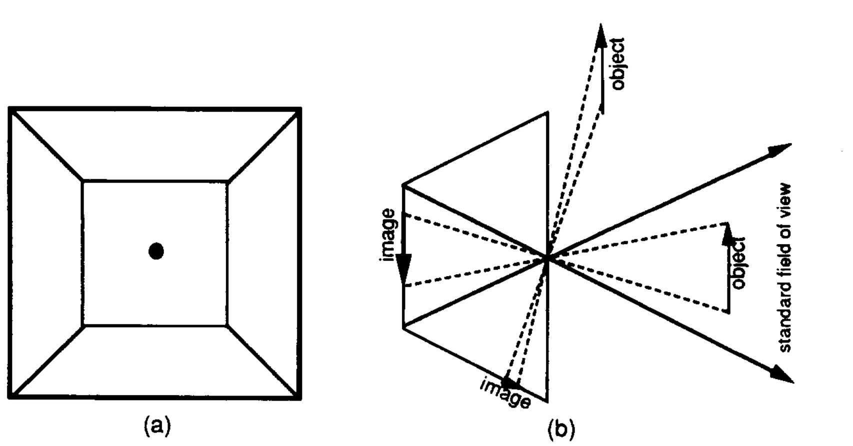

Fig. 8. Peripheral pin-hole model. (a) View from the front (the aperature on the front, larger face is shown, by the dot); (b) side view.

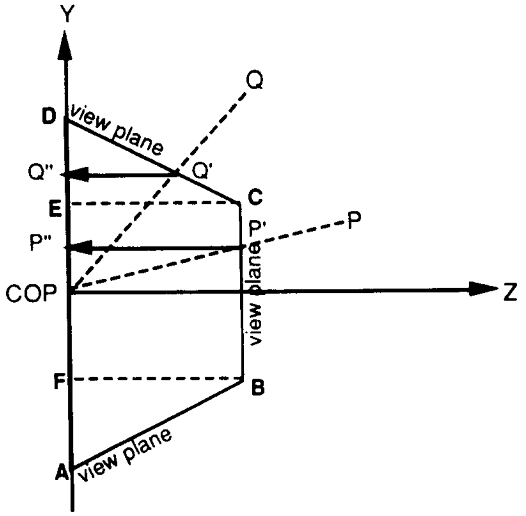

Fig. 9. Peripheral viewing model.

view plane distance locates the front plane ($z = D$ in Fig. 10), and the view plane window ($u_1 < u_2$, $v_1 < v_2$) is the front plane window.

5. IMPLEMENTATION

5.1. *The standard viewing pipeline*

In the standard viewing model there is a pipeline for transformation of a World Coordinate point to the display:

(a) Transform to Viewing Coordinates;
(b) Transform Viewing Coordinates to a canonical view, that is with the clipping planes at 45° to the Z axis, the COP at the origin;
(c) clipping in 3D may be performed at this stage;
(d) Do the projective transformation into 4D homogeneous coordinates (x, y, z, w) (clipping may alternatively be done in 4D at this stage);
(e) Project to 3D, so that (x, y, z, w) becomes $\left(\frac{x}{w}, \frac{y}{w}, \frac{z}{w}\right)$, and render performing hidden surface removal using the z-value (with the z-buffer algorithm for example), with display points $\left(\frac{x}{w}, \frac{y}{w}\right)$.

5.2. *The modified pipeline*

In the new model, the stages are the same, except that matrices are different. The first stage is identical. Without loss of generality, assume that the COP is the origin of viewing coordinates, and that the back plane window is given by opposite corner coordinates (x_1, y_1) and (x_2, y_2). Let $dx = x_2 - x_1$, $dy = y_2 - y_1$, $x_1 + x_2 = y_1 + y_2 = 0$. Similarly, let the front plane window be (u_1, v_1) and (u_2, v_2), with $du = u_2 - u_1$, $dv = v_2 - v_1$, $pu = u_1 + u_2$, and $pv = v_1 + v_2$. Then it is not difficult to show that the matrix R below will transform the situation of Fig. 10, into the canonical model of Fig. 11.

$$R = \begin{pmatrix} \frac{2}{dx} & 0 & 0 & 0 \\ 0 & \frac{2}{dy} & 0 & 0 \\ -\frac{r_x}{D} & -\frac{r_y}{D} & \frac{1}{L} & 0 \\ 0 & 0 & 0 & 1 \end{pmatrix}$$

$$\text{where } L = \left(\frac{dx}{dx - du}\right)D = \left(\frac{dy}{dy - dv}\right)D$$

$$r_x = \frac{pu}{dx}$$

$$r_y = \frac{pv}{dy}$$

$$d = \frac{D}{L} = \frac{dx - du}{dx} = \frac{dy - dv}{dy}.$$

Note that for consistency, the proportion of the image in the periphery must be the same for x and for y, in

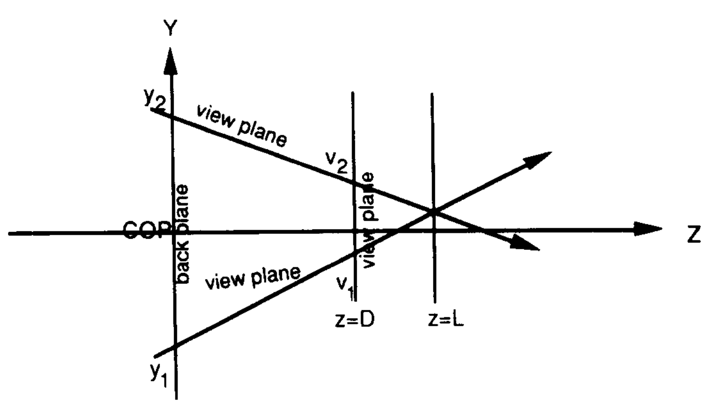

Fig. 10. General peripheral viewing model.

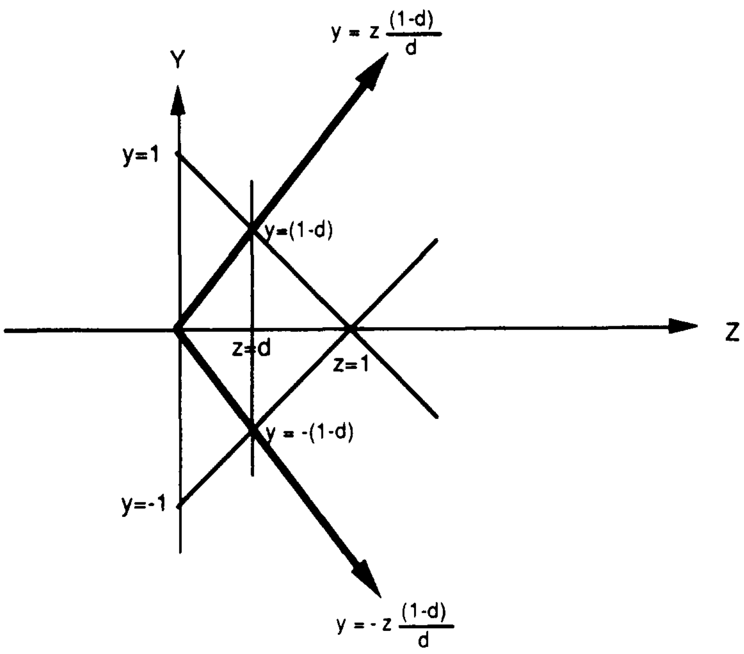

Fig. 11. The canonical peripheral viewing model.

order to define the value of L and d. Note that d is a measure of the proportion of the width (or height) of the final image that is in the periphery.

Clipping to a near clipping plane may be carried out at this stage, or alternatively deferred until the transformation to homogeneous coordinate space.

Imagine now that the entire back plane is pushed back towards $-\infty$ along the Z axis. Figure 12 shows the limit of this process. This is essentially the usual Projection Space of the graphics pipeline, and rendering may be carried out after this stage. It is easy to show that this transformation is achieved with the matrix P, where:

$$P = \begin{pmatrix} 1 & 0 & 0 & 0 \\ 0 & 1 & 0 & 0 \\ 0 & 0 & 1 & r \\ 0 & 0 & -1 & 0 \end{pmatrix}$$

followed by a divide by the homogeneous coordinate. In other words, the transformation from canonical to projection space is given by:

$$x' = \frac{x}{rz}, \quad y' = \frac{y}{rz}, \quad z' = \frac{z-1}{rz}$$

where $r = \frac{1-d}{d}$. The z' values may be used for hidden surface removal in the usual way.

5.3. *2D clipping and projection*

Figure 13 shows a view of the canonical model, where the face $ABCD$ is the front view plane window, and the back plane window is $EFGH$. The point O is the COP, and is on the back plane. Now consider what happens to the various planes under the projective transformation. $ABCD$ becomes the window on the plane $z = -1$, with (x, y) coordinates $(-1, -1)$ and $(1, 1)$ at the corners when the COP moves back to $-\infty$. The planes defined by OAD, ODC, OBC, OAB each become horizontal or vertical: the plane ODC becomes the plane $y = 1$, OAB becomes $y = -1$, OAD becomes $x = -1$ and OBC becomes $x = 1$.

Now consider the planes defined by OCG and OAE. These become the plane defined by $y = x$, and similarly OHD and OBF become the plane $y = -x$. Looked at from the front, the final situation becomes as shown in Fig. 14 (ignore the polygon $abcd$).

Now, from an implementation point of view this is a very useful result. Recall that in projection of a point, if the ray from the point to the COP intersects the front

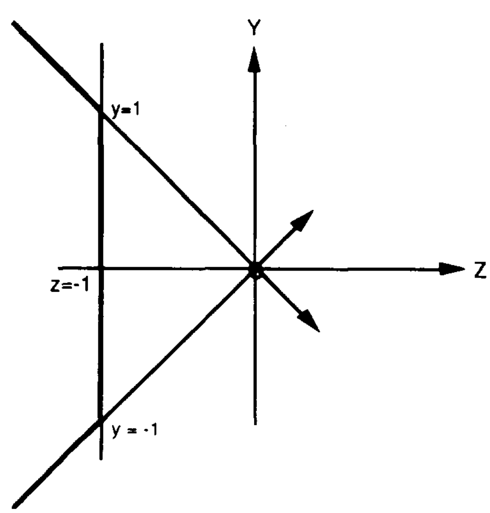

Fig. 12. The space under the projective transformation.

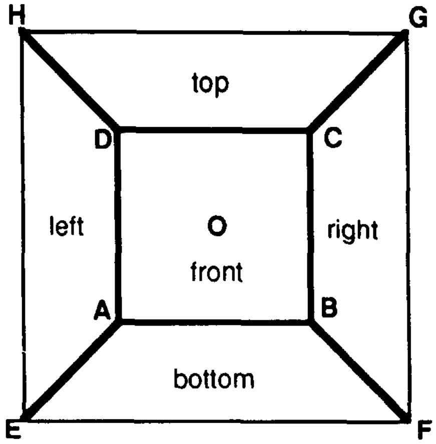

Fig. 13. The canonical peripheral viewing model.

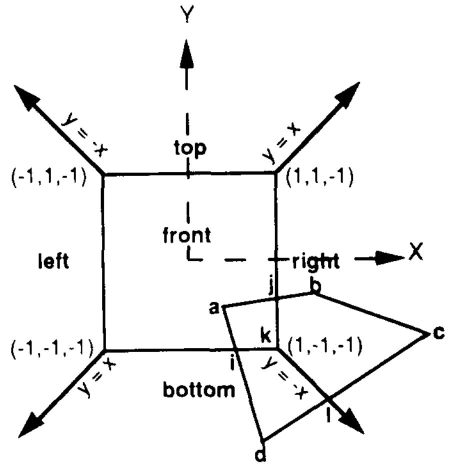

Fig. 14. Front view of projection space.

view plane window $ABCD$, then it is projected as normal. However, if it intersects one of the regions such as $DCGH$ (top) then it is first projected onto that plane, and then there is a parallel projection to the back plane window. In fact the points that project to the left, top, right, and bottom regions are precisely those points in the periphery. Not only are they projected differently to the central points (on the front view plane window) but also may be rendered differently, for example, at a more coarse resolution, or simple shading, or whatever is required.

Given a polygon in the canonical space corresponding to Fig. 13, we would have to clip it in 3D to the planes defined by ODC, OBC, OAB, OAD, ODH, OCG, OBF, and OAE in order to discover the polygon fragments that would project to the left, top, right, bottom, and central regions. However, instead of this, we can transform the polygon to the projection space of Fig. 14, and then clip it to the corresponding regions in 2D. For example, the fragment of the polygon clipped to the front region of this space would project to the $ABCD$ plane of Figure 13, and each of the remaining correspondences holds.

It is relatively straightforward to clip a polygon efficiently in a single pass through its vertices to the regions given in Fig. 14. This can be accomplished using the new space subdivision clipping algorithm for polygons described in [17]. The polygon shown in Fig. 14, *abcd*, would fragment into: *ajki* on the front view plane, *jbclk* on the right plane, and *ldik* on the bottom plane.

Depending on which view plane the fragment is projected to, the formula for projection is different. For example, consider the point (x, y, z) in canonical view space, and suppose that this projects to the front view plane window. The parametric equation of the ray from the origin to the point is $(x(t), y(t), z(t)) = (tx, ty, tz)$ and the plane equation is $z = d$. Hence the intersection point occurs at $t = d/x$, and therefore the intersection point is $\left(\frac{xd}{z}, \frac{yd}{z}, d\right)$ with image on the back plane window $\left(\frac{xd}{z}, \frac{yd}{z}\right)$.

Now consider intersection with the top plane. This has plane equation $y + z = 1$, and therefore at intersection of the ray with the plane, $t = \frac{1}{y+z}$. The image on the back plane is at $\left(\frac{x}{y+z}, \frac{y}{y+z}\right)$. Table 1 gives the results for each of the planes.

6. RESULTS

The new viewing model has been implemented on a workstation prior to an implementation on the ProVision system. Some pictures are shown in Fig. 15a–d. Wire frame drawings are presented because these show more clearly the effects of the viewing model. Figure 15a gives a view just at the entrance to a room. The observer is looking straight ahead, with eye level about half way up the centre of the window on the opposite wall. The reader should focus on this point while looking at these pictures. The FOV for this view is 90°, horizontal and vertical. The image shows what is probably the corner of a desk and some shelves, at the right and left sides of the room.

Figure 15b shows a peripheral view exactly the same scene, with the same viewpoint and FOV in the central region. However, here the value of $d = 0.2$, that is, in both the horizontal and vertical directions, 20% of the

Table 1. Projection of the point (x, y, z) in canonical view space to the back plane.

View plane window	Projection
Top	$\left(\frac{x}{y+z}, \frac{y}{y+z}\right)$
Bottom	$\left(\frac{x}{-y+z}, \frac{y}{-y+z}\right)$
Left	$\left(\frac{x}{-x+z}, \frac{y}{-x+z}\right)$
Right	$\left(\frac{x}{x+z}, \frac{y}{x+z}\right)$
Centre	$\left(\frac{xd}{z}, \frac{yd}{z}\right)$

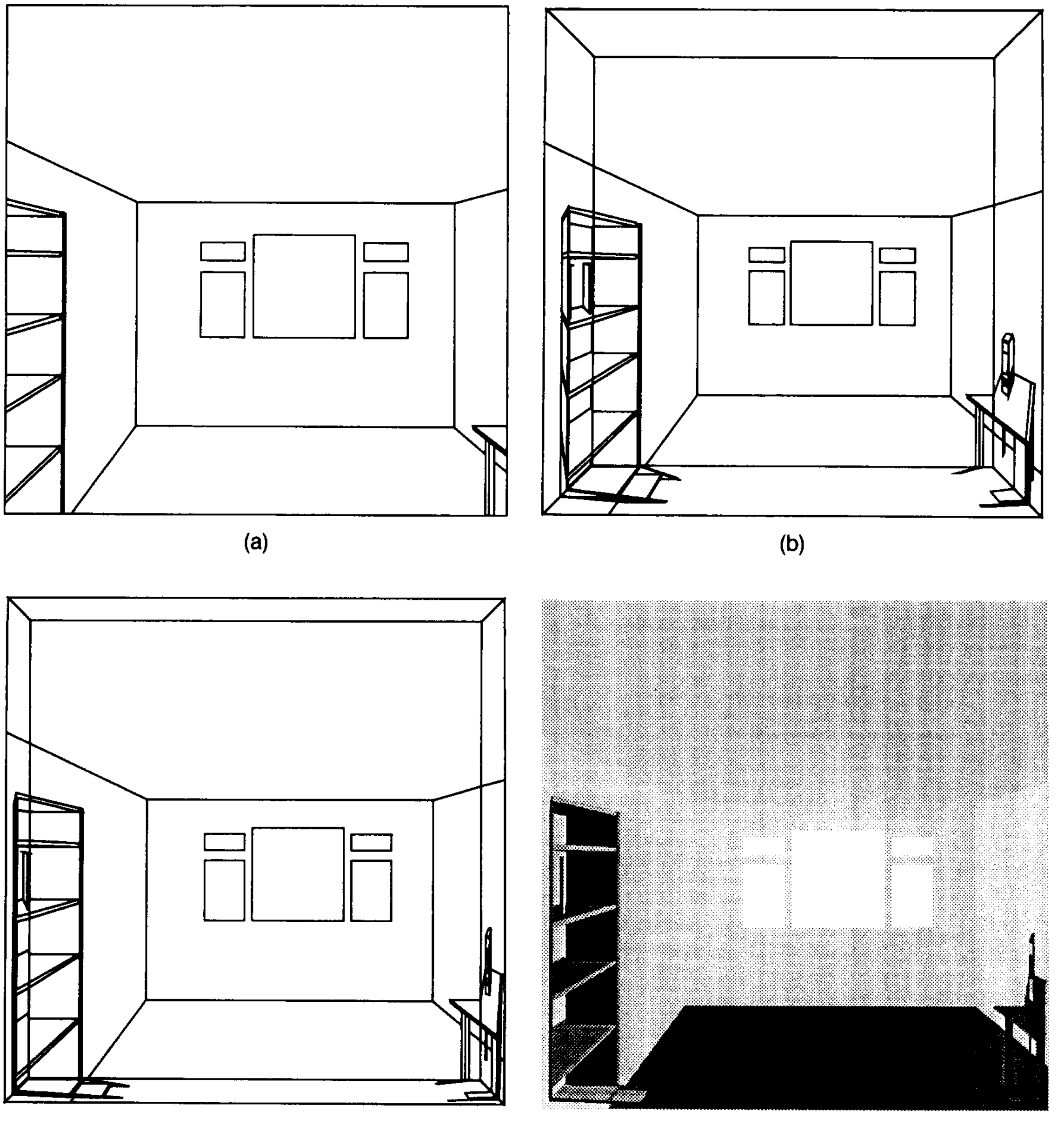

(a) (b) (c) (d)

Fig. 15. (a) Standard view, FOV = 90°; (b) view with a periphery, $d = 1/5$; (c) view with a periphery, $d = 1/10$; (d) shaded view with a periphery, $d = 1/10$.

image is in the periphery. Now all of the information in a 180° FOV is in the image, with distorted perspective of the complete desk and book case around the edges. Figure 15(c) shows the same scene, with $d = 0.1$, a more sensible value. The point is not to get an accurate representation of what is in the periphery, but to show that there is something there, so as to stimulate the observer to look around and get it into the centre of the view.

The wire frame drawings explicitly show the polygons as fragmented into the centre, top, right, bottom, and left regions. Of course, in a shaded image this fragmentation would not be apparent. Figure 15d repeats the same view as Fig. 15c, but now with shading. Note, for example, that the fragmentation of the ceiling is no longer visible.

The point of this method is not to produce static images that are correct when looked at on a screen or photograph. The experience of a participant in an IVE is a dynamic one; there would be a continual optical flow in the peripheral boundary, and events that occur in the periphery would be displayed within that boundary. It is the hypothesis of this research that such peripheral events would stimulate the participant to look in the direction of such events, that would otherwise go unnoticed.

7. CONCLUSIONS

This paper has concentrated on the problem of peripheral vision in IVEs. This is an important issue, since peripheral vision plays an important role in stimulating head and eye movements. The loss of peripheral vision in IVEs may have important consequences for task performance and possibly for presence. The informal experiment carried out in this research suggests that peripheral vision can be stimulated in IVEs, though further work is certainly required on this issue.

An alternative viewing model has been introduced that shows how to compute a peripheral view, and some examples have been shown. This peripheral view contains the standard perspective view in a central region of the image, with a 180° FOV attainable peripherally displayed in a border around the central view. To date this has been implemented on a workstation with the intention of implementing it on a virtual reality system. Whether this particular model is useful in IVEs is a question that must await further implementation and experimental work.

Acknowledgements—We would like to thank Anthony Steed for commenting on an earlier draft of this paper, and Dr. John Patterson for providing information about the visual system. This work is part of a project funded by the London Parallel Applications Centre, a collaborative project for architectural walkthrough, with DIVISION UK Ltd, and Thorn EMI Central Research Laboratories.

REFERENCES

1. M. Bajura, H. Fuchs, and R. Ohbuch, Merging virtual objects with the real world: Seeing ultrasound imagery within the patient. *Comp. Graph.* (*SIGGRAPH*) **26** (2), 203–210 (1992).
2. S. R. Ellis, Nature and origin of virtual environments: A bibliographic essay, *Comp. Syst. Eng.* **2** (4), 321–347 (1991).
3. K. N. Leibovic, *The Science of Vision*, Springer-Verlag, Berlin (1990).
4. A. C. Guyton, *Textbook of Medical Physiology* (8th Ed.), W.B. Saunders, Philadelphia, PA (1991).
5. V. Bruce and P. R. Green, *Visual Perception: Physiology, Psychology and Ecology* (2nd Ed.), Lawrence Erlbam Associates, Hillsdale, NJ (1992).
6. D. Emslie-Smith, C. R. Patterson, T. Scratcherd, and N. W. Read, *Textbook of Physiology* (11th Ed.), Churchill Livingston, London (1989).
7. G. K. Edgar, K. T. Carr, M. Williams, J. Page, and A. L. Clarke, The effects upon visual performance of varying binocular overlap. *Advisory Group for Aerospace Research and Development (AGARD) Conference Proceedings* 517, Helmet Mounted Displays and Night Vision Goggles, 7 Rue Ancelle 92200, Neuilly Sur Seine, France (1992).
8. E. M. Howlet, Wide angle orthostereo. In *Stereoscopic Displays and Applications*, J. O. Merritt and S. S. Fisher (Eds.), International Society for Optical Engineering, Bellingham, WA (1990).
9. M. Slater and M. Usoh, Presence in immersive virtual environments. IEEE Virtual Reality Annual International Symposium (VRAIS), Seattle, WA, 90–96 (1993).
10. M. Slater and M. Usoh, The influence of a virtual body on presence in immersive virtual environments, VR 93, virtual reality international. *Proceedings of the Third Annual Conference on Virtual Reality*, Meckler, London, 34–42 (1993).
11. M. Slater and M. Usoh, *Representation Systems, Perceptual Position and Presence in Virtual Environments*, Presence, Teleoperators and Virtual Environments, MIT Press, Cambridge, MA (in press).
12. M. Deering, High resolution virtual reality. *Comp. Graph.* (*SIGGRAPH*) **26** (2), 195–202 (1992).
13. R. Kalawsy, The science of virtual reality and virtual environments, Addison-Wesley, Reading, MA (1993).
14. ACM, Special Issue: Graphics Standards, *ACM Comp. Surveys* **10**(4) (1978).
15. ISO, 9592 Information processing systems—Computer graphics. *Programmers Hierarchical Interactive Graphics System (PHIGS)—Functional Description*. (See also ANSI, X3.144-1988).
16. J. D. Foley, A. Van Dam, S. Feiner, and J. Hughes, *Computer Graphics: Principles and Practice*, Addison-Wesley, Reading, MA (1990).
17. M. Slater and B. A. Barsky, 2D line and polygon clipping based on space subdivision. *Visual Comp.* (in press).
18. M. H. Pirenne, *Vision and the Eye*, Chapman and Hall, London (1967).